Supporting information

Aliphatic-Bridged Early Lanthanide MOFs: Topological Polymorphism and Excitation-Dependent Luminescence

Pavel A. Demakov, Alexey A. Ryadun, Vladimir P. Fedin

Nikolaev Institute of Inorganic Chemistry SB RAS, 3 Lavrentiev ave., Novosibirsk 630090, Russia

Single crystal X-ray diffraction details

Table S1. Single crystal XRD experiment and refinement details for **1**, **2**$_{Ce}$, **2**$_{Pr}$.

	1	**2**$_{Ce}$	**2**$_{Pr}$
Chemical formula	$C_{30}H_{54}La_2N_2O_{19}$	$C_{50.25}H_{51.25}Ce_2N_{4.75}O_{12.75}$	$C_{50.25}H_{51.25}N_{4.75}O_{12.75}Pr_2$
M_r, g/mol	1024.57	1205.95	1207.53
Crystal system	Triclinic	Monoclinic	Monoclinic
Space group	$P\bar{1}$	$P2_1/n$	$P2_1/n$
Temperature, K	170	292	170
a, Å	9.0209(6)	10.5829(3)	10.5217(4)
b, Å	10.5442(7)	17.9877(5)	17.9353(7)
c, Å	11.8081(6)	13.2388(4)	13.0839(5)
α, °	81.253(5)	90	90
b, °	68.994(6)	98.833(3)	99.054(4)
γ, °	72.993(6)	90	90
V, Å^3	1001.27(12)	2490.28(13)	2438.30(16)
Z	1	2	2
F(000)	514	1208	1212
D(calc.), g/cm^3	1.699	1.608	1.645
μ, mm^{-1}	2.18	1.87	2.04
Crystal size, mm	0.24 × 0.09 × 0.07	0.51 × 0.11 × 0.10	0.35 × 0.10 × 0.07
θ range for data collection, °	$1.9 < \theta < 25.4$	$1.9 < \theta < 25.3$	$2.3 < \theta < 25.4$
No. of reflections: measured/independent/observed [$I > 2\sigma(I)$]	6947 3667 3268	11900 4560 4021	11095 4467 3777
R_{int}	0.0278	0.0206	0.0232
Index ranges	$-10 < h < 10$ $-12 < k < 8$ $-14 < l < 14$	$-12 < h < 12$ $-21 < k < 19$ $-15 < l < 11$	$-12 < h < 12$ $-21 < k < 20$ $-15 < l < 15$
Final R indices [$I > 2\sigma(I)$]	0.0331 0.0790	0.0234 0.0545	0.0235 0.0495
R indices (all data)	0.0396 0.0815	0.0285 0.0569	0.0325 0.0521
Goodness-of-fit on F^2	1.050	1.056	1.027
Largest diff. peak/hole, e/Å^3	2.16/–0.89	0.53/–0.37	0.77/–0.45

Table S2. Single crystal XRD experiment and refinement details for **2**$_{Nd}$, **2**$_{Sm}$, **3**.

	2$_{Nd}$	**2**$_{Sm}$	**3**
Chemical formula	$C_{50.25}H_{51.25}N_{4.75}Nd_2O_{12.75}$	$C_{50.25}H_{51.25}N_{4.75}O_{12.75}Sm_2$	$C_{54}H_{61.33}N_6Nd_2O_{14.67}$
M_r, g/mol	1214.19	1226.41	1317.57
Crystal system	Monoclinic	Monoclinic	Trigonal
Space group	$P2_1/n$	$P2_1/n$	$R\bar{3}$
Temperature, K	170	170	100
a, Å	10.5234(4)	10.4751(4)	37.790(5)
b, Å	17.9568(6)	17.8590(6)	37.790(5)
c, Å	13.0405(5)	12.9892(5)	10.303(2)
α, °	90	90	90
b, °	98.916(3)	98.735(3)	90
γ, °	90	90	120
V, Å^3	2434.44(16)	2401.77(15)	12742(4)
Z	2	2	9
F(000)	1216	1224	5982
D(calc.), g/cm^3	1.656	1.696	1.545
μ, mm^{-1}	2.18	2.49	2.12
Crystal size, mm	0.79 × 0.14 × 0.11	0.33 × 0.11 × 0.09	0.70 × 0.20 × 0.20
θ range for data collection, °	2.0 < θ < 25.4	2.0 < θ < 25.3	2.7 < θ < 26.7
No. of reflections: measured/independent/observed [$I > 2\sigma(I)$]	8388 4471 3895	10347 4404 3813	13340 5107 4819
R_{int}	0.0343	0.0251	0.0323
Index ranges	–12 < h < 7 –21 < k < 13 –15 < l < 14	–12 < h < 12 –21 < k < 17 –10 < l < 15	–45 < h < 45 –25 < k < 45 –12 < l < 10
Final R indices [$I > 2\sigma(I)$]	0.0317 0.0743	0.0253 0.0551	0.0393 0.0939
R indices (all data)	0.0382 0.0794	0.0326 0.0575	0.0417 0.0950
Goodness-of-fit on F^2	1.072	1.051	1.093
Largest diff. peak/hole, e/Å^3	1.09/–1.10	0.68/–0.58	1.19/–1.35

PXRD supplementary data

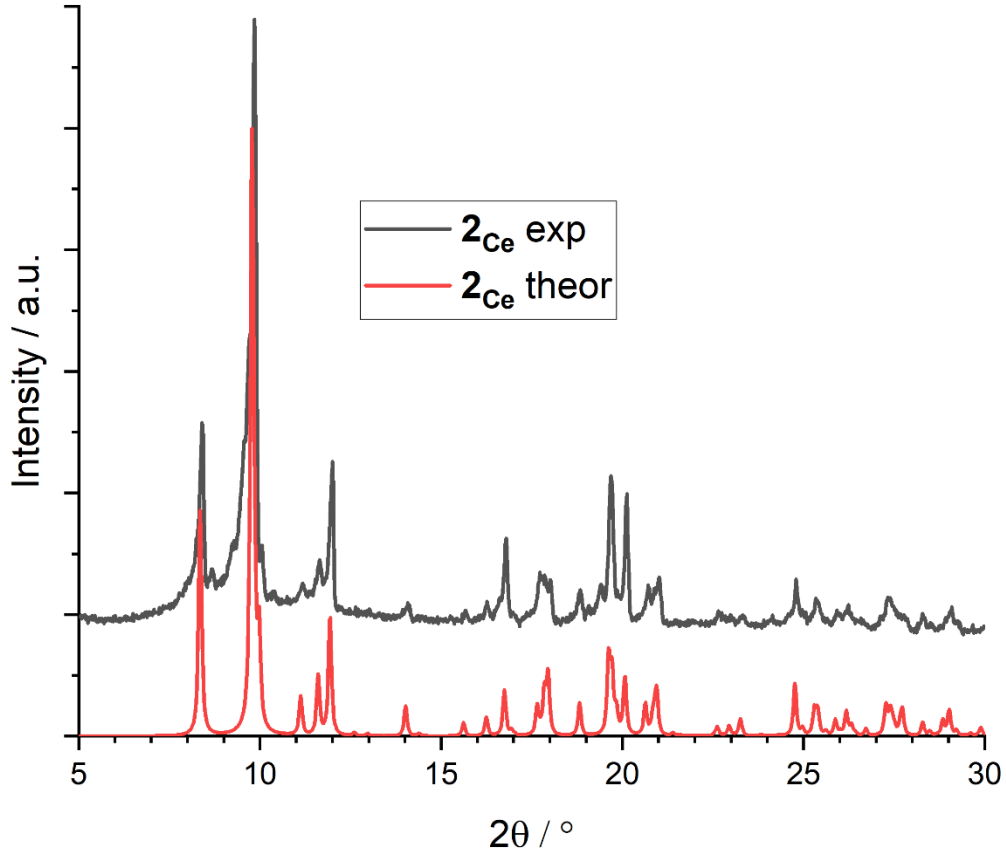

Figure S1. Experimental (black) and theoretical (red) PXRD patterns for **2**$_{Ce}$.

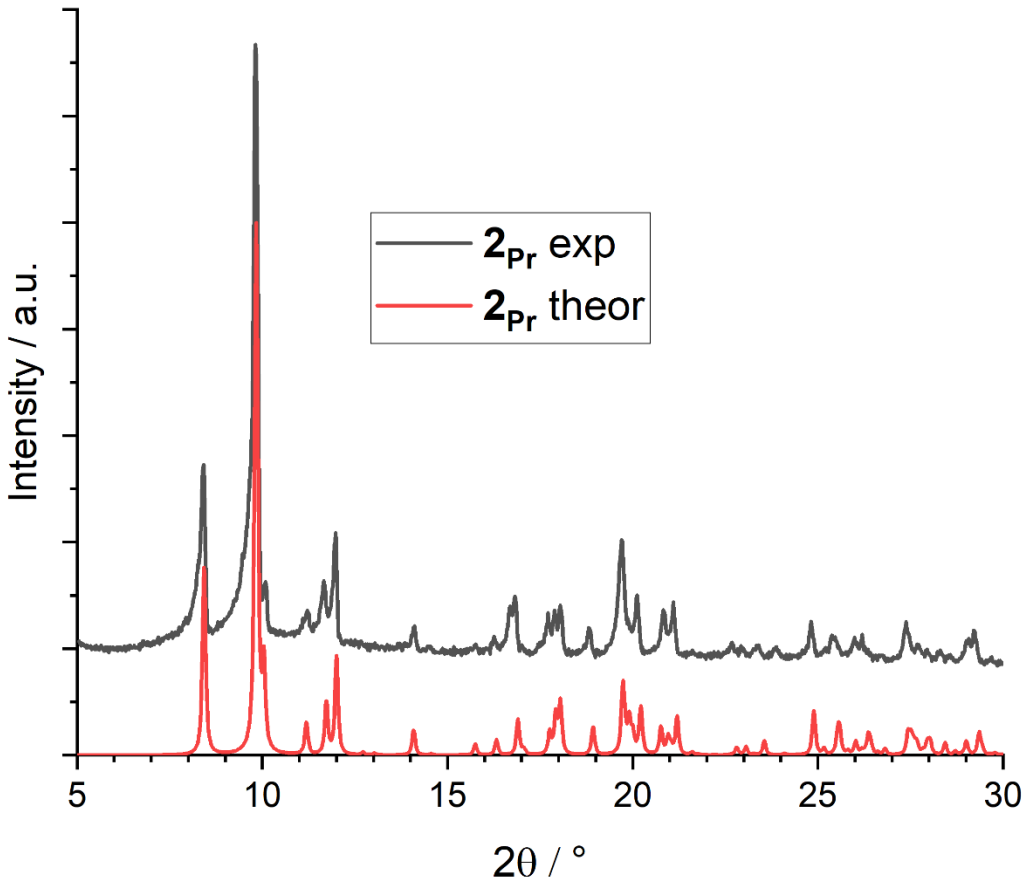

Figure S2. Experimental (black) and theoretical (red) PXRD patterns for **2**$_{Pr}$.

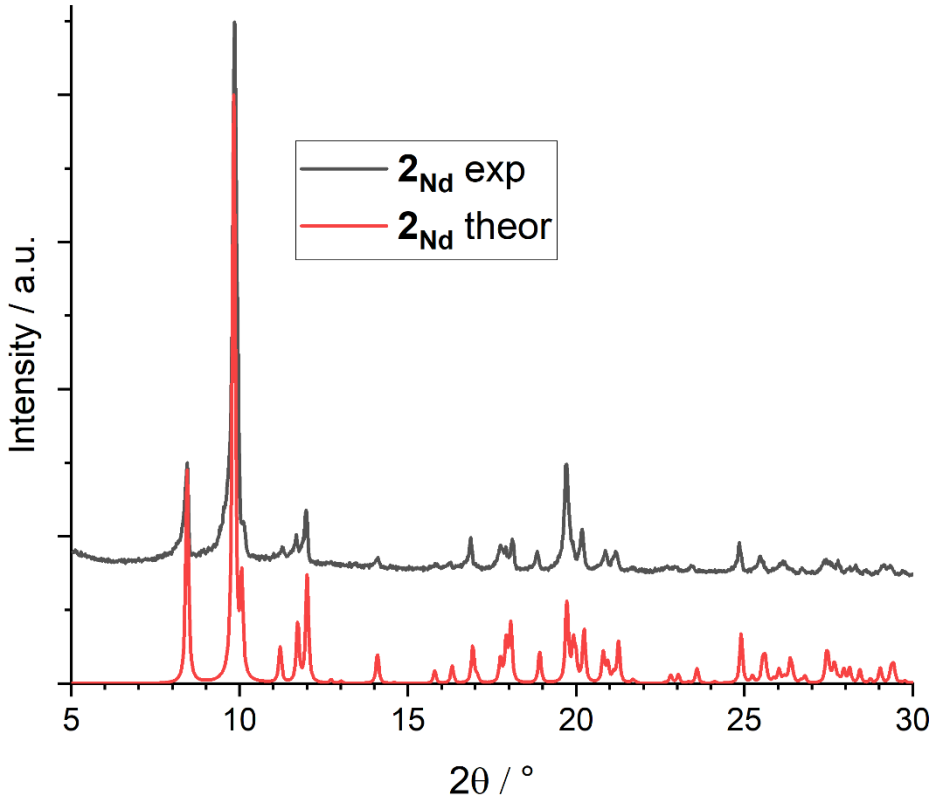

Figure S3. Experimental (black) and theoretical (red) PXRD patterns for **2**Nd.

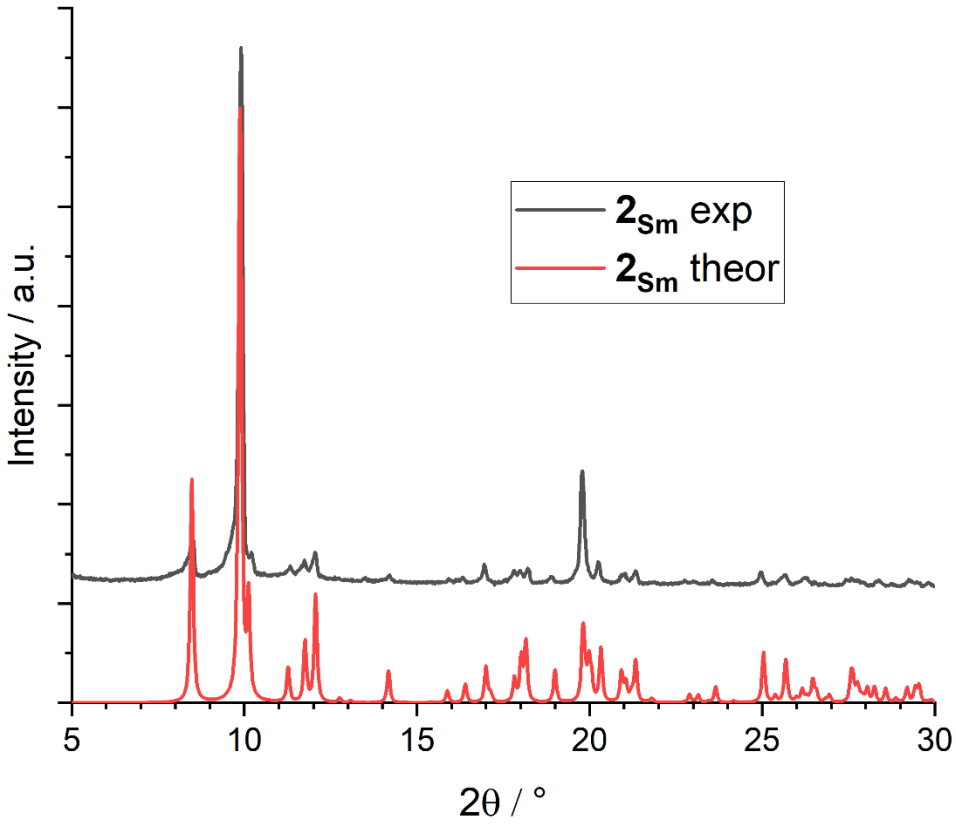

Figure S4. Experimental (black) and theoretical (red) PXRD patterns for **2**$_{Sm}$.

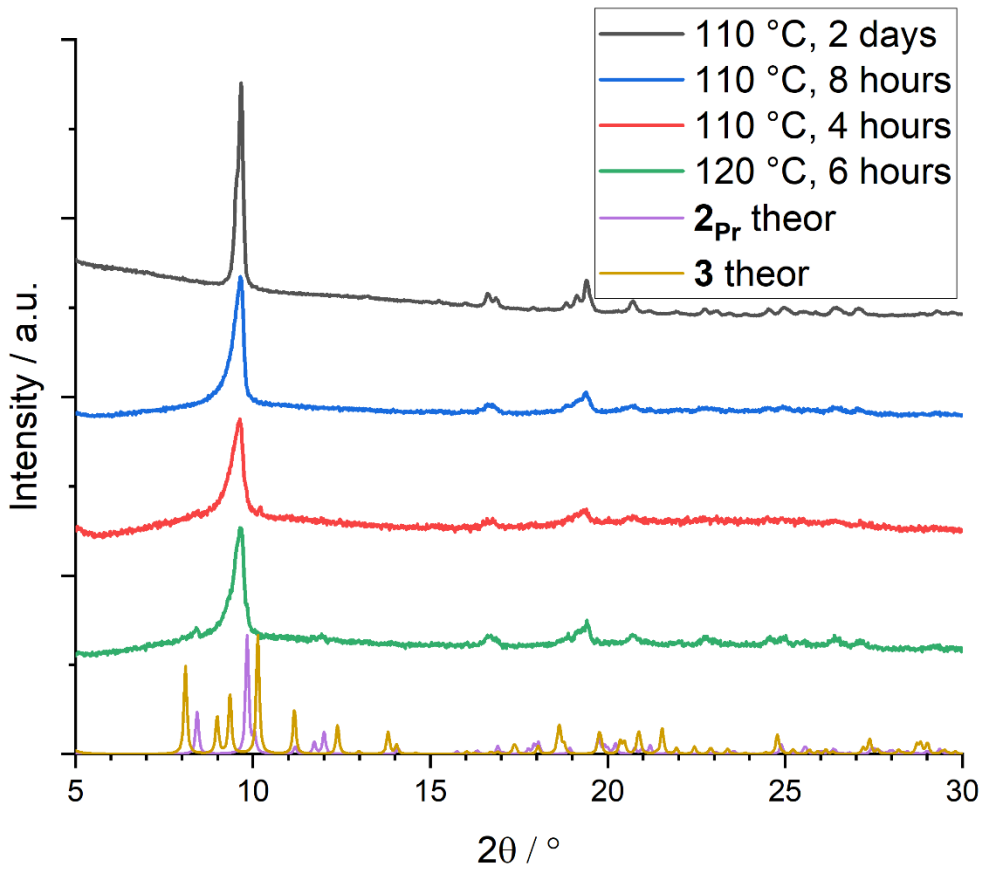

Figure S5. PXRD patterns for **2**$_{Pr}$ temperature- and time-screening syntheses.

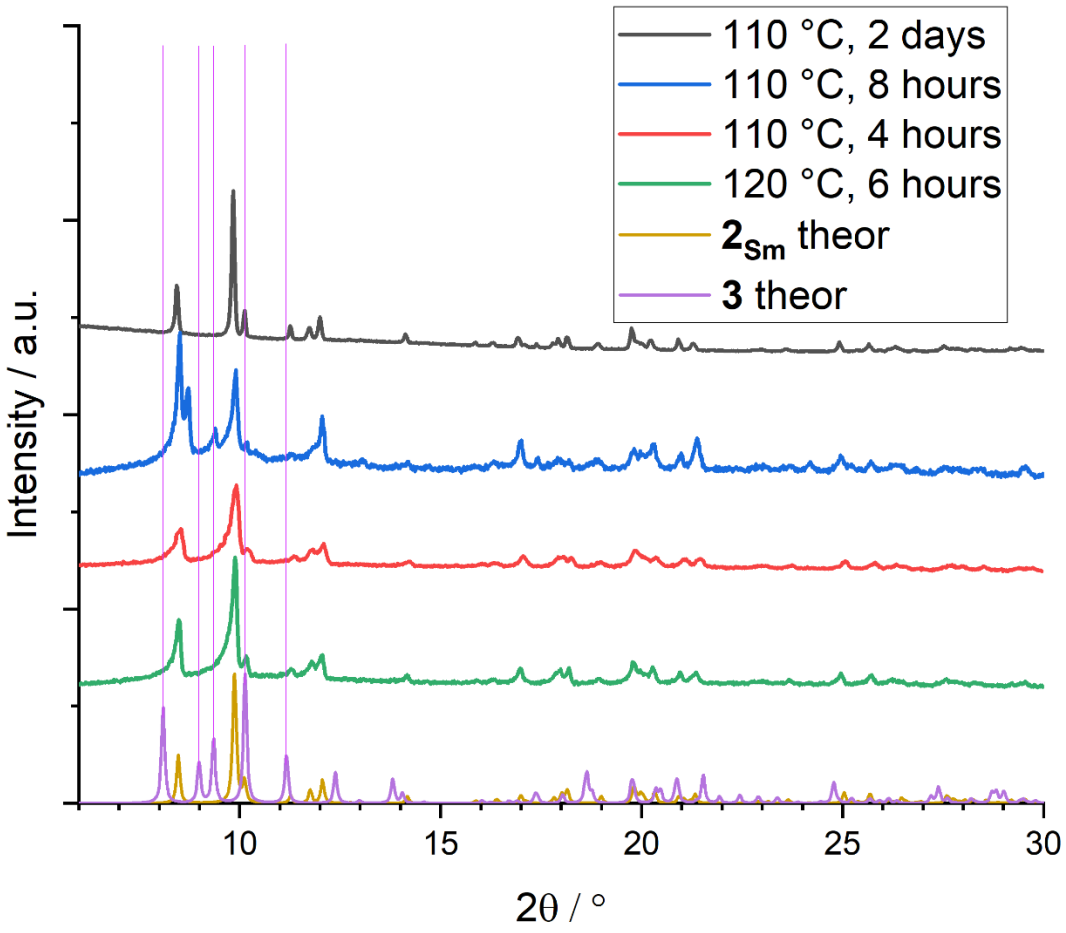

Figure S6. PXRD patterns for **2**$_{Sm}$ temperature- and time-screening syntheses. Magenta lines show positions for lowest-angle reflections in theoretical **3** structure.

Description of **1'** compound

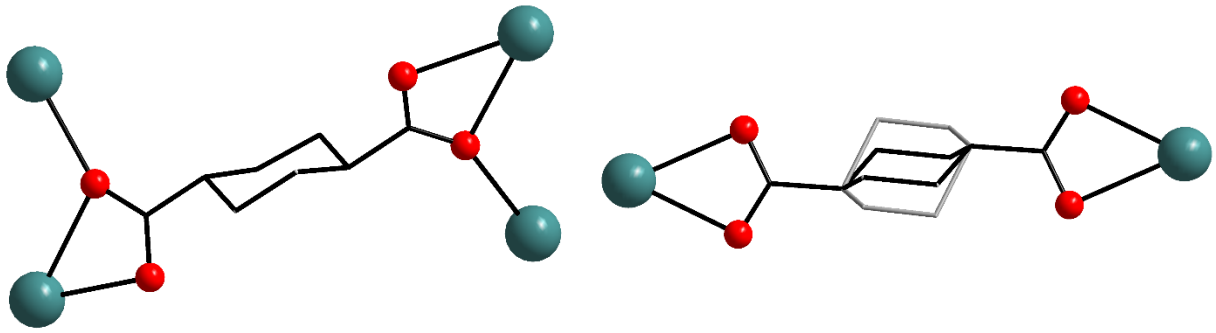

a b

Figure S7. Coordination modes of (k^2,k^1;k^2,k^1)-chdc ligand (**a**) and (k^2;k^2)-chdc ligand (**b**). Cyclohexane ring in (**b**) is disordered over two positions, the second position is shown grey.

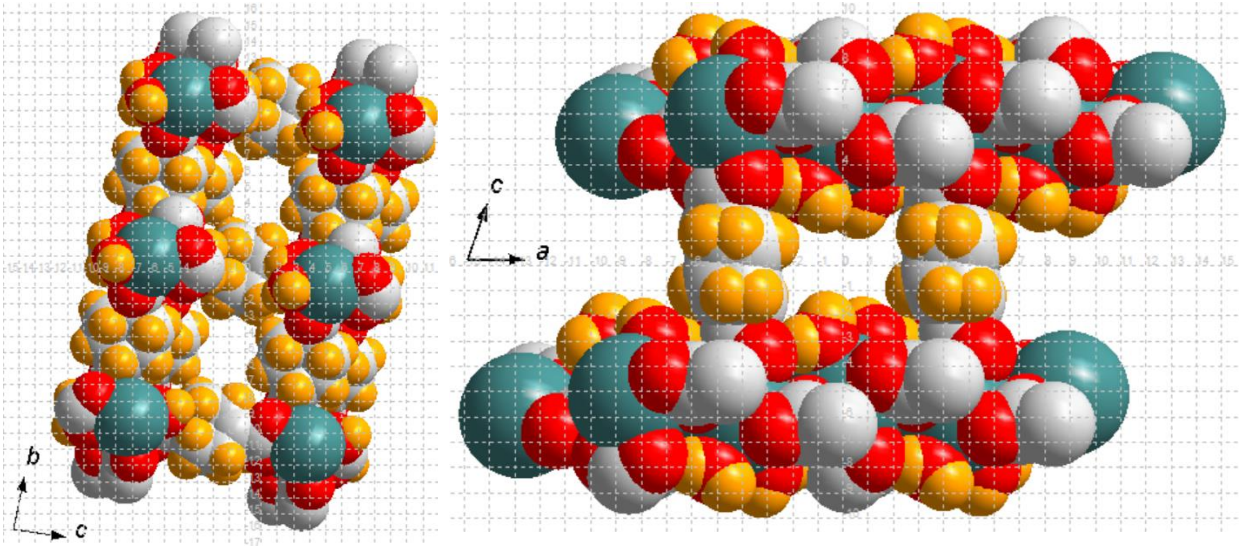

a b

Figure S8. Space-filling representation of channels in the coordination framework of **1**. Grids with 1 Å step are imposed on both the figures.

PXRD pattern obtained for the filtered sample of **1'** shows the disappearance of most of the peaks presented in the theoretical pattern. However, a detailed analysis of the indexed diffractogram (see figure S1a) gives necessary insights into the nature of molecular mobility in the crystal structure of **1**. First two reflections appearing at *ca*. 8.0° and 8.8° on the theoretical diffractogram contain the reflections of crystallographic planes with (0 0 1) and (0 1 0) Miller indexes, respectively. The corresponding interplanar distances are mainly controlled by (κ^2;κ^2)-chdc ligand (fig. 2c) and (κ^2,κ^1;κ^2,κ^1)-chdc ligand, respectively. On the experimental diffractogram, the intensity of (0 0 1) reflection is significantly decreased and the peak is shifted to $2\theta \approx 8.1°$, while (0 1 0) reflection remains intact. At larger angles, the only intensive peak at $2\theta \approx 17.6°$ presents, which corresponds to (0 2 0) plane. Such analysis suggests that desolvation of **1** when stored in air leads to a contraction of [$La_2(H_2O)_4(chdc)_3$] 3D framework along *c* crystallographic axis, which is attributed to the (κ^2;κ^2)-chdc ligand. On the contrary, the framework structure retains along *b* axis, which corresponds to more robustly coordinated (κ^2,κ^1;κ^2,κ^1)-chdc. These observations are also supported by a larger space which is accessible for (κ^2;κ^2)-chdc molecular motions (see figure 2c) instead of (κ^2,κ^1;κ^2,κ^1)-chdc ligands, closely packed to each other (see figure S9b).

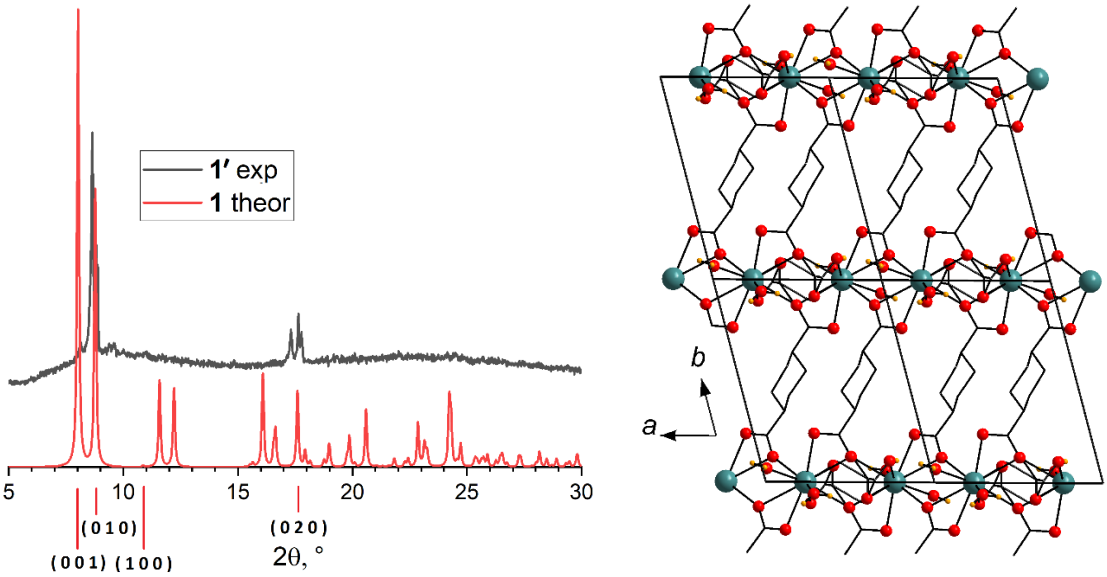

a b

Figure S9. Experimental (black) PXRD pattern for **1′** and theoretical (red) one for **1** (a). View along *c* crystallographic axis in **1** (b). Atom colors correspond to figure 3 in the manuscript, H atoms of chdc ligand and guest molecules are not shown.

IR spectrum of **1′** (Fig. S11) contains characteristic absorption bands for water O–H vibrations, cyclohexane ring and DMF methyl group C(sp^3)–H vibrations, DMF C=O vibrations and COO group antisymmetric and symmetric stretchings. The absence of aromatic C(sp^2)–H absorption bands in 3075-3060 cm^{-1} region, as well as the absence of strong bands at *ca*. 1583, 1534 and 850 cm^{-1} confirm the absence of phenanthroline in **1′** in any (coordinated or guest) form, fully matching crystal structure data obtained for its parent compound **1**.

According to TG (fig. S10), first 13 % weight loss step for **1′** occurs at *ca*. 280 °C, which corresponds well to the evaporation of the residual coordinated solvents. The second weight loss step occurs at *ca*. 505 °C and is apparently attributed to the decomposition of La-chdc coordination framework.

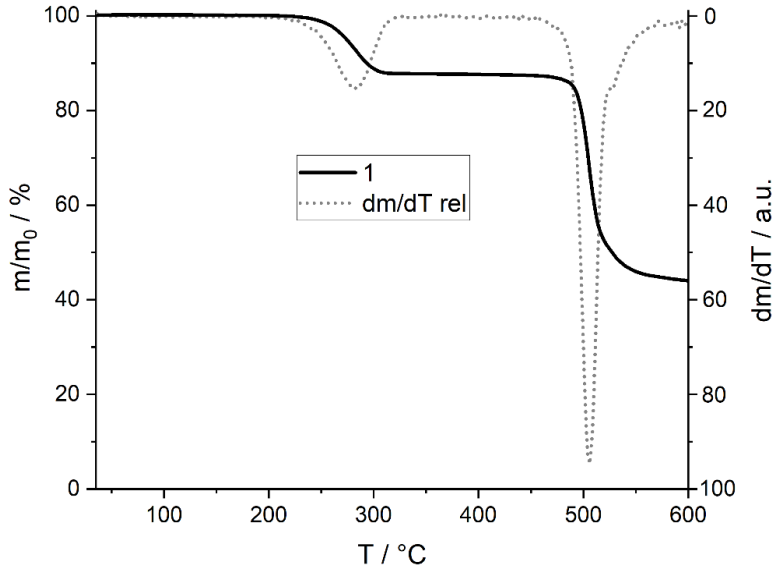

Figure S10. TGA pattern and relative dm/dT curve for the sample **1′**.

Bond lengths in metal environment

Table S3. Selected bond lengths in **2**$_{Ln}$ and **3**.

Bond	**2**$_{Ce}$	**2**$_{Pr}$	**2**$_{Nd}$	**2**$_{Sm}$	**3 (Nd)**
Ln–O(κ^2-COO)	2.530(2) 2.553(2)	2.508(2) 2.526(2)	2.502(3) 2.516(3)	2.478(2) 2.481(3)	2.471(3) 2.490(3)
Ln–O(κ^1,κ^1-COO)	2.437(2) 2.487(2)	2.418(2) 2.4706(19)	2.402(3) 2.456(3)	2.374(2) 2.422(2)	2.414(3) 2.437(3)
Ln–O(κ^2,κ^1-COO)	2.4172(18) 2.572(2) 2.6151(17)	2.3965(19) 2.553(2) 2.5803(18)	2.383(2) 2.540(3) 2.573(2)	2.351(2) 2.495(2) 2.551(2)	2.413(3) 2.561(3) 2.565(3)
Ln–N(phen)	2.639(14) … 2.70(3)	2.600(12) … 2.70(3)	2.581(15) … 2.67(3)	2.552(12) … 2.61(2)	2.617(4) … 2.71(4)

Infrared spectra and TGA details

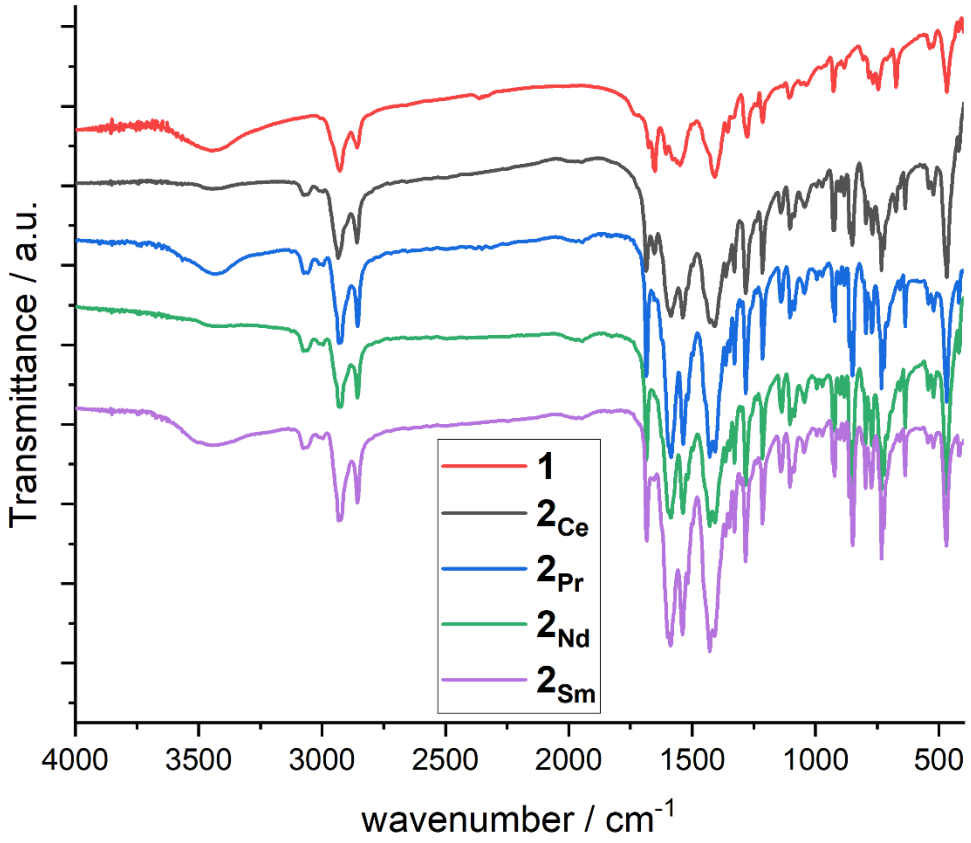

Figure S11. Infrared spectra for **1′** and **2**$_{Ln}$.

Table S4. Details on TG decomposition steps of **1′** and **2**$_{Ln}$.

Com-pound	Solvent loss			Framework decomposition			Ln_2O_3 calcd. residue / %
	T range / °	Max.loss T / °	Weight residue / %	T start / °	Max.loss T / °	Weight residue / %	
1′	220 – 320	280	87	~ 460	505	44	36
2$_{Ce}$	25 – 400	-	95	~ 400	470, 495	43	27 (28 for CeO_2)
2$_{Pr}$	230 – 430	-	95.5	~ 410	470, 485, 505	34	27
2$_{Nd}$	250 – 440	-	96	~ 415	495, 510	38	28
2$_{Sm}$	250 – 450	-	96	~ 415	490, 505	39	28

Luminescence supplementary data

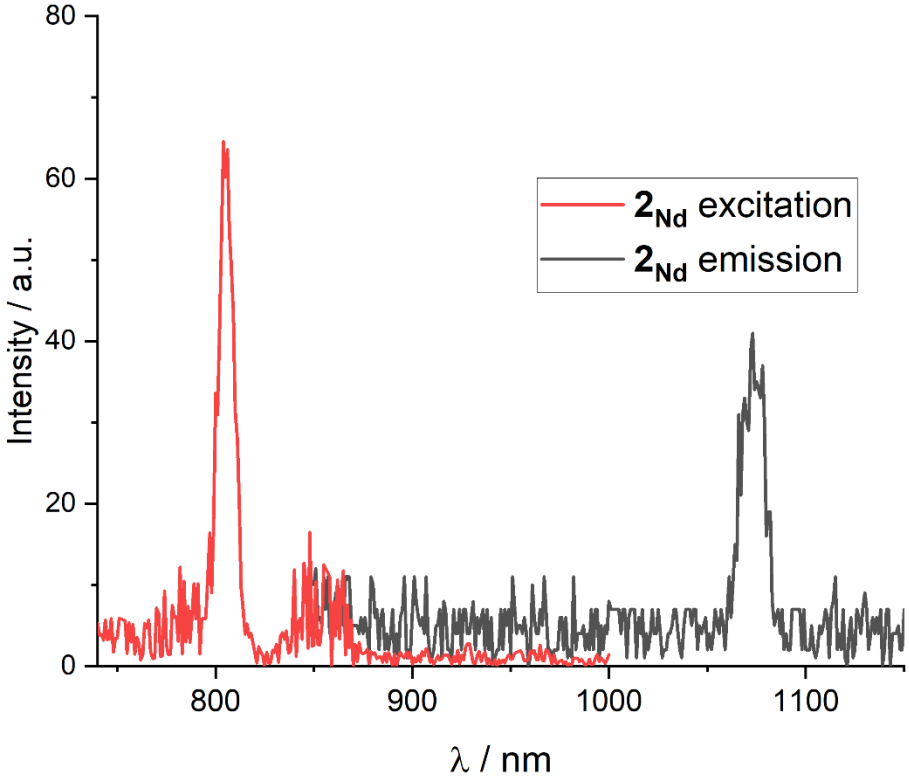

Figure S12. Excitation (red) spectrum for **2**$_{Nd}$ at λ_{em} = 1077 nm and emission (black) spectrum for **2**$_{Nd}$ at λ_{ex} = 804 nm.

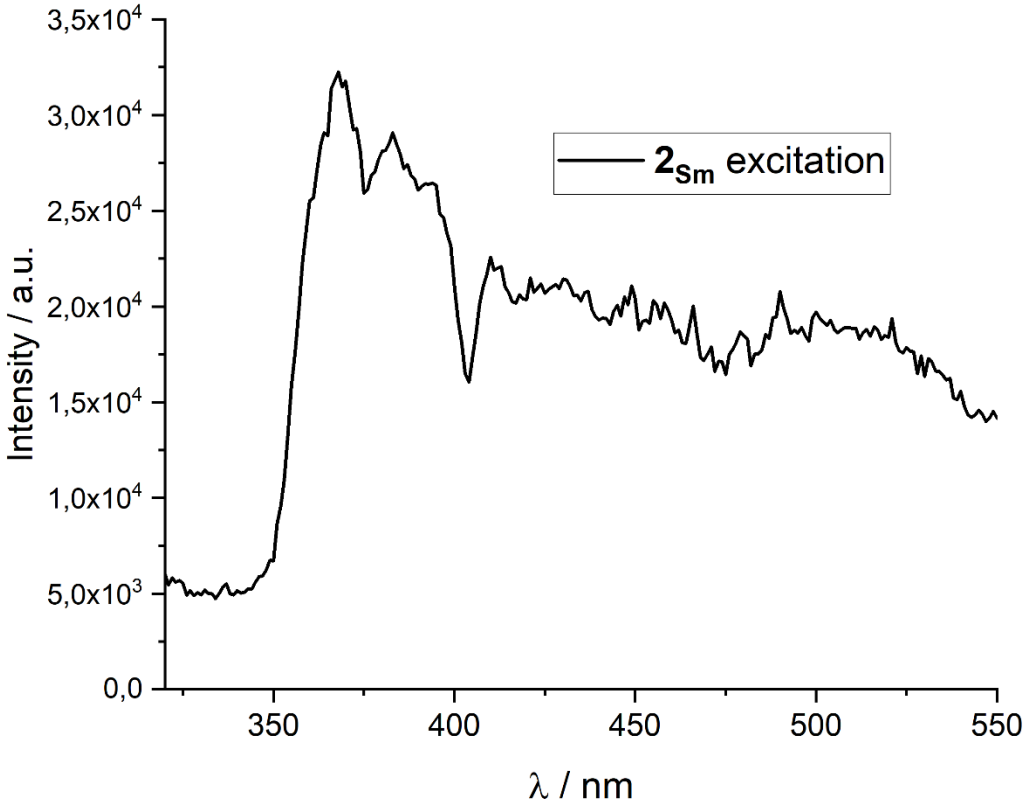

Figure S13. Excitation spectrum for **2**$_{Sm}$ at λ_{em} = 580 nm